Discharge Characteristics of the Spherical Inertial Electrostatic Confinement (IEC) Device

George H. Miley, *Fellow, IEEE*, Yibin Gu, John M. DeMora, Robert A. Stubbers, Timothy A. Hochberg, Jon H. Nadler, and Robert A. Anderl

***Abstract*—The University of Illinois inertial electrostatic confinement (IEC) device provides 10^7 2.5 MeV D-D neutrons/second when operated with a steady-state deuterium discharge at 70 kV [1]. Being compact and lightweight, the IEC potentially represents an attractive portable neutron source for activation analysis applications [2]. The plasma discharge in the IEC is unique, using a spherical grid in a spherical vacuum vessel with the discharge formed between the grid and the vessel wall, while the -70 kV grid (cathode) also serves to extract high-energy ions. Two key features of the IEC discharge are discussed: 1) the breakdown voltage characteristics as a function of pressure–grid/wall distance (pd), and 2) the formation of ion "microchannels" that carry the main ion flow through grid openings.**

***Index Terms*—Hollow cathode discharge, inertial electrostatic confinement (IEC), microchannels, neutron source, plasma breakdown, spherical cathode.**

I. Introduction

ION-INJECTED inertial electrostatic confinement (IEC), originally proposed by Farnsworth [3], the inventor of electronic television, was first studied experimentally by Hirsch in the 1970's [4]. Recently, University of Illinois researchers developed a unique single-grid version of the IEC, and found an unusual "STAR" mode discharge involving current "microchannels" that lead from openings in the grid to the center of the spherical discharge. There are alternate types of IEC's, e.g., Hirsch [4] used ion-gun injectors, Barnes *et al.* used a triple-grid design [5], and Bussard has proposed a hybrid magnetic–electrostatic version [6]. Compared to the present single-grid devices, these designs generally operate at lower pressures due to added electron injection, but much of the basic physics carries over [1]. The present paper discusses basic experimental studies of the plasma discharge characteristics in this single-grid IEC, along with computer simulations used to obtain further insight into the microchannel phenomenon.

II. Voltage Breakdown

The current–voltage and pressure–voltage characteristics of the single-grid-type IEC have been studied experimentally. These characteristics are shown to differ from those of equivalent "conventional" solid-cathode discharges that operate in this pressure–electrode separation product, pd, range [7], [8]. This difference is attributed to the fact that the transparent IEC grid cathode allows ion flow on a chord that connects the opposite sides of the spherical grid by passing through the center of the device.

A. The IEC Devices

Two spherical IEC devices were used in these experiments, one having a 30-cm diameter vacuum chamber (IEC-A) and another having a 61 cm diameter chamber (IEC-B). As shown in Fig. 1, each device consists of a spherical cathode grid mounted concentrically within a grounded spherical vacuum vessel, which serves as the anode. The system is maintained at a constant pressure of 5–15 mtorr by bleeding gas into the chamber through a leak valve, with the vacuum pump running. The plasma discharge is then initiated by increasing the cathode voltage until breakdown occurs, typically at 5–50 kV.

The grid-type cathodes employed in the IEC devices [Fig. 1(b)] are constructed of 0.8 mm diameter stainless-steel wire, spot welded into open spherical grids having 85–90% geometric transparencies. Various sizes and types of cathode grids were used in these experiments, as indicated in Table I. Note that B2 is a solid stainless-steel sphere instead of a wire grid. The solid-sphere-type cathode was included in the experiments for comparison with data from other "conventional" solid-cathode discharge devices reported in the literature.

A 0–100 kV, 0–25 mA dc power supply was used to power the IEC. However, due to voltage limitations on the cathode feedthroughs, the maximum voltage was limited to approximately 40 kV in present experiments.

B. V Versus pd Measurements

In order to determine how the applied voltage V depends on pd and current I, two types of measurements were taken: I versus V at various values of pd, and the striking (or "breakdown") voltage V_s versus pd. The latter plot corresponds to the traditional "Paschen curve" plot. However, note that for the IEC geometry, d refers to the radial distance from the grid to the vacuum chamber wall. The I–V characteristics of the devices are shown in Fig. 2. The current essentially remains zero as V is increased until the discharge is initiated at V_s, after

Manuscript received April 1, 1996; revised April 11, 1997.

G. H. Miley, Y. Gu, J. M. DeMora, R. A. Stubbers, and T. A. Hochberg are with the Fusion Studies Laboratory, University of Illinois, Urbana, IL 61801 USA (e-mail: g-miley@uiuc.edu).

J. H. Nadler is with the Department of Physics, Richland Community College, Decatur, IL 62521 USA.

R. A. Anderl is with LITCO, Idaho National Engineering and Environmental Labatory, Idaho Falls, ID 83415 USA.

Publisher Item Identifier S 0093-3813(97)05533-1.

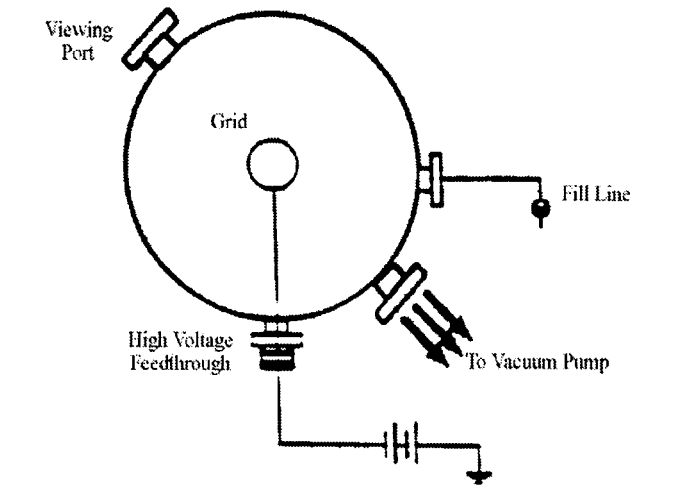

(a)

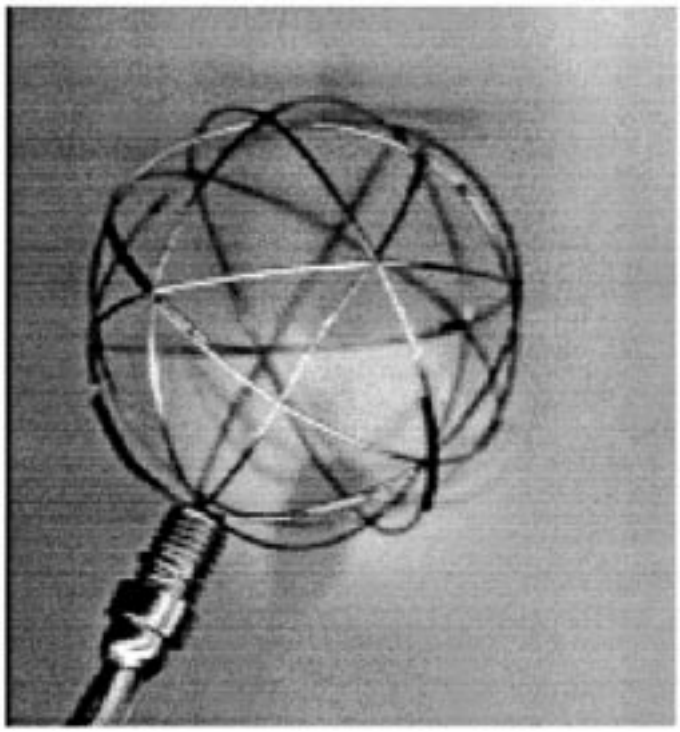

(b)

Fig. 1. Configuration for a typical single-grid IEC device and spherical wire grid. (a) Spherical IEC device. (b) Typical grid cathode used in IEC.

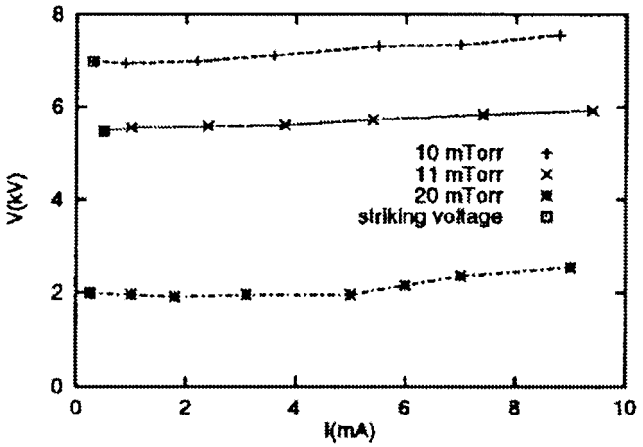

Fig. 2. Voltage versus current in IEC-A using grid A1 and hydrogen fill gas. As noted, the striking and operating voltages nearly coincide.

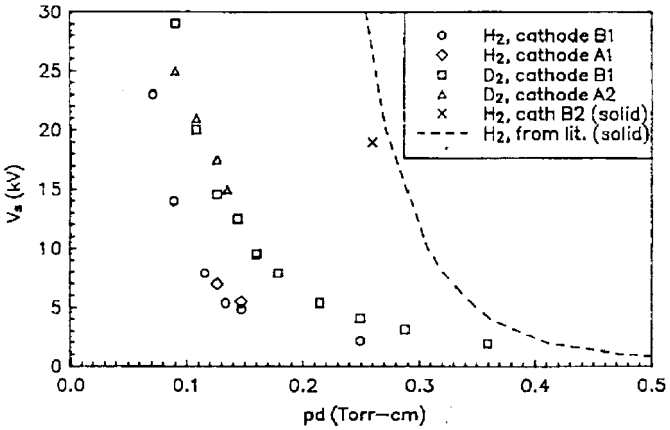

Fig. 3. Striking voltage versus pd for grid-type cathodes versus solid cathodes.

which, to a first approximation, the voltage remains constant as the current is further increased. As noted in the Introduction, similar behavior is observed for the solid-cathode discharge in this pressure range, but the actual voltage values are quite different.

A plot of V_s versus pd is shown in Fig. 3 for a hydrogen discharge in IEC-A with various grids, including results for a solid spherical cathode plus a curve for a "conventional" hydrogen discharge with a plate-type solid cathode [8]. Although the latter is for a plane-parallel discharge, it matches the data from solid-cathode B2 relatively well. For a fixed V_s, the value of pd is seen to be about three times higher for both the spherical and the planar solid-cathode discharges than for the transparent grid-type cathode discharges. As discussed later in more detail in connection to cases where holes are drilled in the solid cathode, this difference is attributed to the flow of ion current through the transparent grid cathode versus the solid sphere which prevents directed flow on a chord passing through the center of the device.

As is clearly visible in the photograph of a typical discharge shown in Fig. 4, for pd below about 0.5 torr·cm, the discharge consists of current-carrying microchannels, which appear as spokes emanating from the holes in the cathode grid [1]. This unique discharge phenomenon, discovered at the University of Illinois, is termed the "Star" discharge mode. These microchannels radiate both outward from the cathode to the anode, and inward to the center of the sphere where they form a bright central plasma "core." This implies that the intense microchannel discharge occurs between the anode and the local plasma volume encompassed by *holes* in the cathode, i.e., that microchannels seek the regions of highest grid transparency. Thus, the discharge characteristics should depend on an "effective" grid transparency (t), as opposed to the geometric transparency. That is, t accounts for the higher transmission probability of ions in the microchannels

Fig. 4. Digital photograph of the Star mode, taken through the IEC viewport. The microchannels and dense "core" plasma are clearly visible.

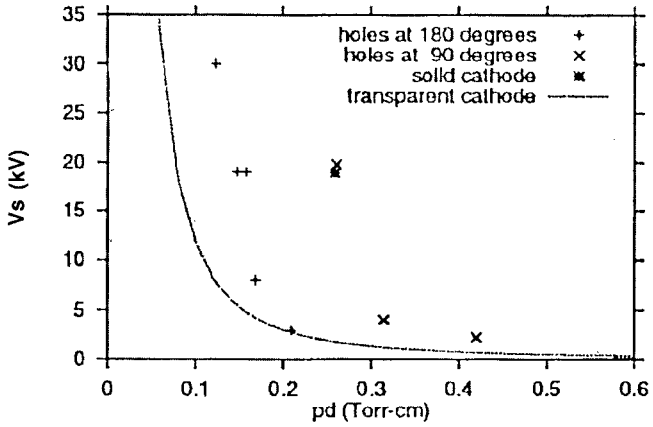

Fig. 5. Striking voltage V_s versus pd for solid cathodes including cases with holes at various orientations. A curve for transparent wire grids based on (1) is included.

versus a uniform "sheet"-like flow. Microchannel losses $(1-t)$ are determined by the frequency with which ions scatter out of the microchannel and onto a path that leads them into a grid wire. At high voltage, the scattering of energetic ions is relatively infrequent. Thus, t is expected to be significantly larger than the geometric transparency. Essentially, ions in the microchannels are "guided" through the grid, minimizing interception of the grid wires.

These microchannels are not initially formed by constricting E–M forces. Rather, as illustrated by computer simulations described later, they are created through a geometric "self-selection" process. That is, ions born with trajectories hitting grids within a few passes are quickly eliminated, while those passing repeatedly through grid holes survive, leading to increased ionization ("births") along these favored trajectories.

In order to test this the effective transparency hypothesis for microchannels, cathode A1 was covered with aluminum foil, except for two 2-cm diameter holes located 180° apart. Spokes now emanated from both holes, and, as shown in Fig. 5, the discharge characteristics for this configuration were similar to those of a transparent cathode, despite the very low geometric transparency of the two-hole cathode. The foil was then replaced, and two new holes were cut 90° apart. While the *geometric* transparencies of these two cathodes are equal, due to the formation of microchannels, the *effective* transparency t of the first grid is high, while that of the second is essentially zero. Although the striking voltages (V_s) for this second configuration were well defined, once initiated, the discharges were unstable and appeared qualitatively different from discharges using transparent cathodes. As shown in Fig. 5, the values of V_s for the 180° hole cathode fall close to that for a solid electrode, considerably higher than for the 90° hole case.

In summary, the discharges using a cathode with high effective transparency, such as the 180° hole-type cathode, behave much like transparent-type wire-cathode discharges, even if the geometric transparencies differ greatly. In sharp contrast, the discharges using the cathode with low effective transparency behave as solid-cathode discharges. Thus, we conclude that the discharge characteristics are primarily a function of the effective, rather than the geometric transparency of the cathode.

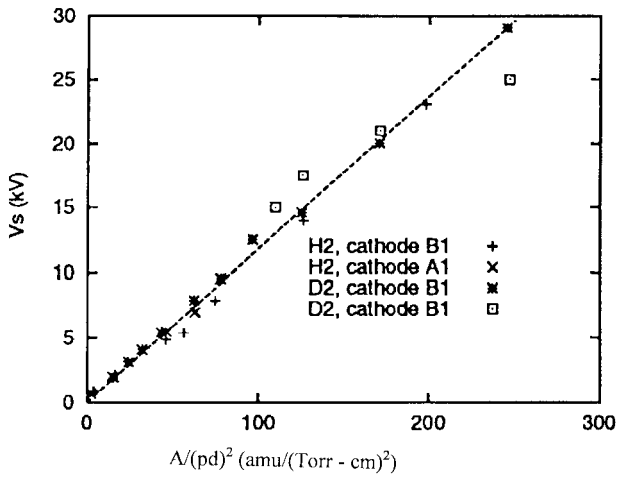

Fig. 6. Plot of the striking voltage V_s versus A/pd^2 for two different gases and various grids.

C. Scaling of Results

An empirical scaling law has been derived [9] by noting that a straight line is obtained if the striking voltage data from Fig. 3 are plotted versus the parameter $A/(pd)^2$, as shown in Fig. 6. Here, A, the atomic mass of the gas species, accounts for the use of various gases. This results in a simple scaling law for these IEC discharges, namely,

$$V_s \approx \frac{0.118A}{(pd)^2} \qquad \text{kV} \cdot (\text{torr} \cdot \text{cm})^2/\mu\text{m}. \tag{1}$$

Since, as shown earlier in Fig. 2, $V \sim V_s$, (1) also provides a good estimate of the operating voltage as well as the breakdown value. Note that (1) also predicts the behavior of the discharge using cathode A1 reasonably well, even though the radius R of this cathode is half that of the other grids. Thus, the discharge characteristics are at most a weak function of R so the radius is not included as a parameter in (1). Further studies are required to accurately define the R dependence.

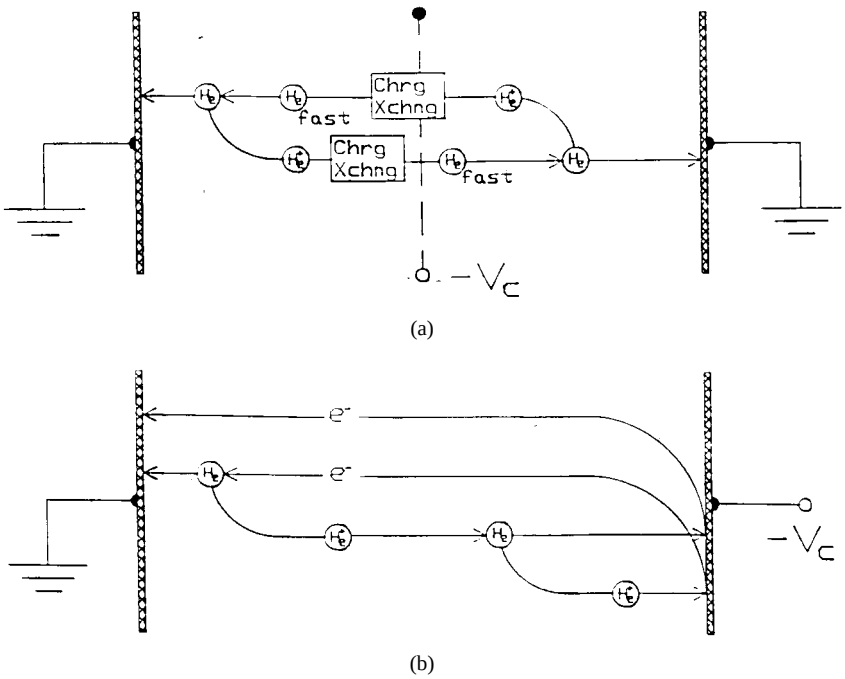

Fig. 7. Comparison of current flow processes in the IEC versus a "conventional" solid-cathode discharge. (a) Ion charge-exchange ("chrg xchng") neutral flow in the case of a transparent cathode, cf. the IEC. (b) Ion, electron flows in a solid-cathode discharge.

D. Monte Carlo Modeling

These various effects have also been studied computationally. A Monte Carlo-type computer model of the discharge mechanism has been developed wherein, as shown in Fig. 7, ion currents play a role similar to electron currents in a standard discharge while charge exchange processes are also incorporated [8], [9]. Thus, the basic ion–electron flow processes included in the code, illustrated conceptually in Fig. 7(a), are to be contrasted to the flows in a solid cathode shown in Fig. 7(b). Ion flow, significantly "enhanced" by fast charge-exchange neutrals, plays a unique role in the IEC transparent cathode case. Microchannel effects are *indirectly* included in the Monte Carlo code by assigning the probability of an ion striking the grid to represent the effective transparency. (In contrast, the SIMION code, described next, employs trajectory calculations to study microchannels *explicitly*.) Results for probabilities ranging from 90 to 99% are included in the Paschen curve plot of Fig. 8, along with experimental data for the various grids of Table I, all with geometric transparencies on the order of 90% or less. The code result with an effective transparency of 99% provides the best fit to the experimental data. This is consistent with the experimental hole-type solid electrode results, and with the conclusion from those experiments that the discharge characteristic is determined by the effective, rather than the geometric transparency. Consequently, these results add confidence to the effective transparency concept, and support the concept that ion, charge-exchange-neutral flows play a fundamental role in current flow in the IEC.

TABLE I
SPHERICAL CATHODE 5 USED IN THE IEC EXPERIMENT

Device/Grid	Diameter (cm)	Construction (Geometric Transparency)
IEC-A		
A1	3.7	wire grid, 85%
A2	7.5	wire grid, 90%
IEC-B		
B1	15	wire grid, 89%
B2	15	hollow sphere, 0%

III. SIMULATION OF MICROCHANNELS

Simulations of the Star mode have also been made using SIMION, an electric field and ion trajectory program developed at the Idaho National Engineering and Environmental Laboratory (INEEL) [10]. SIMION's earlier uses have largely been to model various ion focusing equipment. Electrodes in SIMION are defined point-by-point, and then the program solves Laplace's equation with a finite-difference method to determine the electric potentials created by the electrodes. SIMION uses these potentials to calculate the forces on ions and determine their trajectories. This code does not determine the electric potentials produced by a plasma itself. However, estimates of plasma effects, mainly manifest by distortion of the potential surface in grid holes, indicates that the change in microchannel trajectories (versus those closer to the grid which result in losses anyway) is small.

Fig. 9 shows a sample plot of the ion trajectories in the single-grid IEC. Here, the tightly packed region of ion trajectories in the hollow cathode region closely resemble the ion microchannels of the Star mode. Charge-exchange effects are not included either. In effect, the trajectories calculated represent the combination of fast ion and neutral transport, but neglect losses due to fast neutral escape. While this omission introduces an error in the number of ion recirculations, i.e., in ion losses calculated, the general features of trajectory paths,

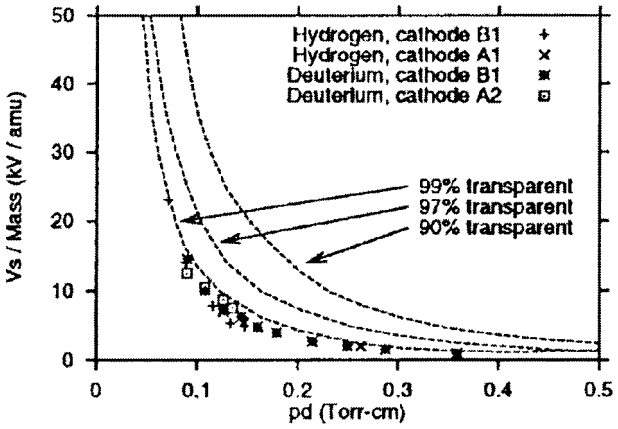

Fig. 8. Calculated Paschen curves for various *effective* transparencies (t) compared to data for grids with *geometric* transparencies $\leq 90\%$. The $t =$ 99% curve provides the best fit.

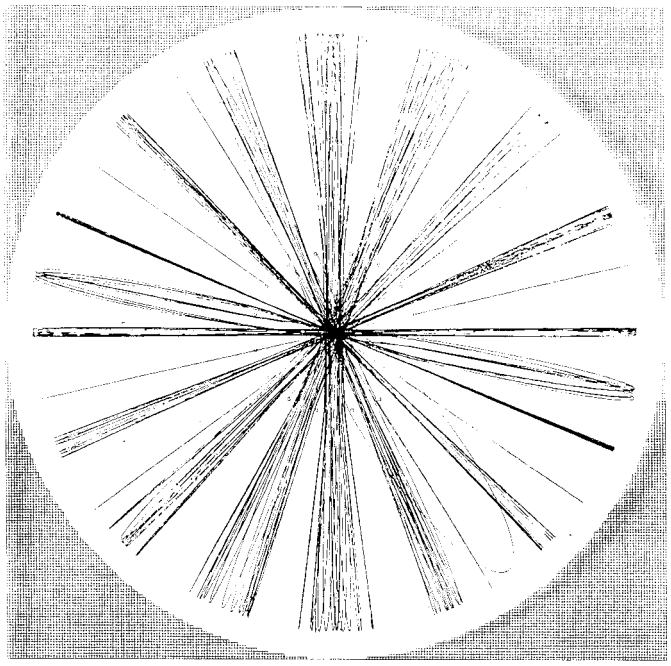

Fig. 9. SIMION calculation of ion paths in the IEC. The trajectory "bundles" resemble microchannels while a dense plasma "core" is formed by intercepting trajectories at the center of the sphere (the shaded outer region defines the chamber wall).

a major objective of these calculations, are not drastically affected.

A. Microchannel Formation

The graphical output of SIMION adds further insight into the phenomenon involved in microchannel formation [11]. The grid cathode produces concave equipotential surfaces in the grid opening, whose shapes are due to the potential of the individual grid wires. These surfaces defocus ions as they approach the grid from the outside. But once an ion enters the grid and passes to the opposite side, it approaches convex potential surfaces which refocus the ion toward the center of the microchannel as it exits the grid. The net result of this phenomenon is that ions that do not initially collide with the grid wires, and do not pass so close to the grid wire that their trajectories are significantly distorted, continue to travel within the microchannel trajectory. Thus, these are the only ions that survive multiple passes ("self-selection"). Subsequent ionization is enhanced along microchannels, further amplifying the effect.

Microchannels are preferentially filled with ions born near the chamber wall (anode), where the electric potential is greater and the perturbation of the electric field due to the grid wires is small. Conversely, if an ion starts near the grid, where a smaller electric potential accelerates it toward the center, the ion may have insufficient momentum as it passes through the grid to avoid signification attraction by the wire; hence, a deflection of its trajectory occurs. If this happens, the ion will be deflected away from the center of the microchannel, and will either collide with the grid or go into an orbit that lies outside the microchannel, and eventually will be lost to a grid. Since such ions are rapidly lost, the majority of ions in the microchannel have higher energies. Correspondingly, these ions have originated (are "born") near the chamber wall. This mechanism provides further "self-selection," and results in a relatively narrow energy spread for the ions in the microchannels.

Fig. 10 further illustrates the significance of the starting (birth) point of the ions. The ions shown earlier in Fig. 9 start near the wall, and form microchannels similar to the experimental observations. In contrast, in Fig. 10, the ions start close to the grid. In the latter case, the ions do not form separate and distinct microchannels; instead, they travel in large, loop-like orbits, and are quickly lost by collision with the grids. These trajectories are similar to those obtained by Moses [12], who used Mathematica to plot ion trajectories where, again, plasma potential effects were neglected. His simulations concentrated on ions born close to the grid, which resulted in their defocusing. Consequently, he suggested that a second focusing grid was needed to maintain the microchannels. Since the present case with ions born closer to the wall reproduces the experimentally observed microchannels, the complication of a second, refocusing grid does not appear necessary. It remains an interesting option, however.

B. Ion–Grid Collision Studies

There are three different ways that an ion can collide with a grid wire in SIMION. The first is to run directly into the wire without passing through the center of the chamber. The second method is to pass through the grid a few times without following a microchannel, then colliding with a wire. The third way is to pass through the center core a few times while remaining in one microchannel before colliding with a wire. Some ions can also follow a microchannel indefinitely in SIMION (in which case a subroutine stops the circulating ion after a certain period of time). In the actual case, collisions, including charge exchange will remove the ion from the microchannel.

Table II shows how many ions collided with the grid and the manner in which they collided. These data are for a 91% geometric transparent grid at -30 kV. Results in Table II

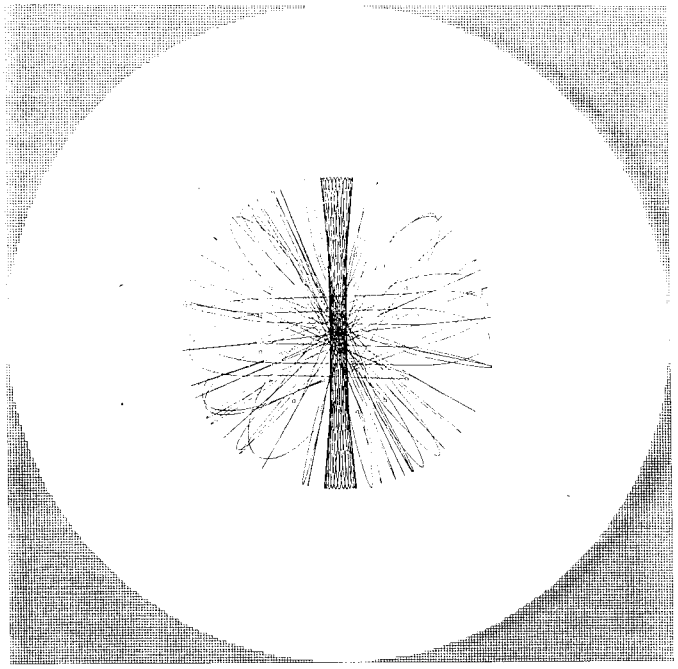

Fig. 10. SIMION plots of ion trajectories where ions born near the grid fail to form discrete microchannels.

TABLE II
HISTORIES FOR HIGH- AND LOW-ENERGY IONS

Ion Beam Location	Ion History	High-energy ions (26 keV)	Low-energy ions (12 keV)
Leaves microchannel	Ion collides directly with grid in first pass	8.8%	8.8%
	Ion not in microchannel collides with grid	19.2%	25.6%
Remains in a microchannel	Leaves channel and collides with grid after several passes	28.8%	55.2%
	Remains in microchannel for many passes	43.2%	10.4%

confirm that the ion distribution in the microchannels favors high-energy ions (cf. 43% of the multipass ions are 26 keV ions) compared to the low-energy (12 keV) ions that start near the grid. (While the absolute values of the percentages shown in Table II will be affected by charge losses, the trends predicted are not expected to be changed.)

For the typical case shown in Table II, about 9% of both high- and low-energy ions are directly lost to the grid without recirculating through it. In addition, 19–25% do not follow microchannel trajectories, and are soon lost to the grid. About 71% of the high-energy ions follow microchannels, of which 60% (cf. 43% of all high-energy ions in and out of microchannels) recirculate freely without striking grids.

In contrast, the fraction of low-energy ions in microchannels that recirculate for multiple passes is only 15% (cf. 10% of the total in and out of microchannels). These results are consistent with the earlier observation that higher energy ions born near the anode (chamber wall) have a better chance of survival and are responsible for the microchannel phenomenon.

These observations suggest that increasing the ion density in the microchannels will increase the fraction of high-energy ions, in turn increasing the fusion rate. One way of achieving this goal is to optimize the grid design, i.e., grid/wall radius ratio, transparency, and grid-wire-to-hole-size ratios. Such an optimization is under study, both experimentally and using SIMION.

C. Summary—Trajectory Studies

The microchannels of the Star discharge mode are formed by a natural selection process if sufficient gradient occurs in the potential surface between the grid openings, creating microchannels. Then ions passing near the grid are deflected and lost, while those near the center of the opening perform multiple passes. This requirement sets limits on the grid design required to create the Star mode. Ions born near the chamber wall (anode) are also favored since they reach the grid with a higher velocity so that their trajectories are less perturbed by the local distortion due to the grid wires. As a result of the multiple passes, additional ions are formed in the microchannel path, increasing the current density in the microchannel in a "bootstrap-like" fashion.

IV. SUMMARY AND CONCLUSIONS

Experiments and simulations described here, employing the unique Star discharge mode involving microchannels discovered at the University of Illinois, have enhanced understanding of the physics of the single-grid-type IEC. Specifically, it has been shown that discharges in the Star mode are governed by the effective, rather than the geometric grid transparency. Further, the formation of microchannels is explained by a "natural" selection process associated with defocusing of non-channel ions by the grid potential surface distortion and favoring higher energy ions born near the anode.

Present single-grid IEC devices, capable of providing 10^7 neutrons/second steady state with a simple, rugged, low-capital-cost device, are of strong interest for various nondestructive evaluation and neutron activation analysis applications [2]. Further study of both the physics and engineering of these devices is necessary, however, in order to ensure long-lifetime operation with minimum maintenance. The extension to higher neutron yields is also under study in order to further expand the range of applications.

ACKNOWLEDGMENT

The assistance of other members of the IEC group at Illinois is appreciated. Helpful discussions with R. Hirsch (R. H. Assoc.), R. W. Bussard (MC2 Corp.), J. Hartwell (INEL), and R. Nebel and D. Barnes (LANL) are gratefully recognized. The use of SIMION was made possible by its author, D. A. Dahl (INEL).

REFERENCES

[1] G. H. Miley, J. Javedani, R. Nebel, J. Nadler, Y. Gu, A. Satsangi, and P. Heck, "Inertial-electrostatic confinement neutron/proton source," in *Proc. 3rd Int. Conf. Dense Z-Pinches*, M. Haines and A. Knight, Eds., AIP Conf. Proc. 299. New York: AIP Press, 1994, pp. 675–689.

[2] R. A. Anderl, J. K. Hartwell, J. H. Nadler, J. M. DeMora, and R. A. Stubbers, "Development of an IEC neutron source for NDE," in *Proc. 16th IEEE/NPSS Symp. Fusion Eng.*, G. H. Miley and C. M. Elliott, Eds. Piscataway, NJ: IEEE, 1996, pp. 1482–1485.
[3] P. Farnsworth, "Electric discharge device for producing interactions between nuclei," U.S. Patent 3 258 402, June 28, 1966.
[4] R. Hirsch, *J. Appl. Phys.*, vol. 38, p. 4522, 1967.
[5] D. C. Barnes, R. A. Nebel *et al.*, "Inertial electrostatic confinement experiments at low working pressure," Rep. NTTR-101, prepared under Contract DAAK70-93-C-0038 U.S. Army, Nambe Tech Corp., Santa Fe, NM.
[6] R. W. Bussard and N. A. Krall, *Fusion Technol.*, vol. 26, pp. 1326–1336, 1994.
[7] A. Von Engel, *Electric Plasmas: Their Nature and Uses.* London, U.K.: Taylor and Francis, 1983, p. 125.
[8] S. Brown, *Introduction to Electrical Discharges in Gases.* New York: Wiley, 1966.
[9] T. A. Hochberg, "Characterization and modeling of the gas discharge in a SFID neutron generator," M.S. thesis, Dept. Nucl. Eng., Univ. Illinois at Urbana–Champaign, 1992.
[10] D. Dahl, INEEL, private communication, 1995.
[11] J. M. DeMora, R. A. Stubbers, and R. A. Anderl, "Study of ion microchannels and IEC grid effects using the SIMION code," in *Proc. 16th IEEE/NPSS Symp. Fusion Eng.*, G. H. Miley and C. M. Elliott, Eds. Piscataway, NJ: IEEE, 1996, pp. 1486–1489.
[12] R. Moses, "Enhancing IEC performance with focusing grids," presented at the Phys. Spherical Continuous Inertial Fusion Workshop, LANL, Santa Fe, NM, Jan. 1995.

George H. Miley (M'72–SM'80–F'87) is a Professor of Nuclear Engineering, Electrical and Computing Engineering, and is a Director of the Fusion Studies Lab at the University of Illinois, Urbana-Champaign. He is well known for this research on advanced fuel fusion and innovative approaches for fusion energy confinement. The IEC research described here is a result of his interest in Philo Farnsworth's original concepts for electrostatic confinement and "poissors." The research is part of an experimental–theoretical program that he initiated to reinvestigate these concepts.

Yibin Gu received the B.S. degree in electrical engineering and the M.S. degree in nuclear engineering from the University of Illinois, Urbana-Champaign. He is currently working toward the Ph.D. degree in electrical engineering on potential structures in the spherical IEC devices.

John M. DeMora received the B.S. degree in nuclear engineering with emphasis on health physics and safety from the University of Illinois, Urbana-Champaign, in 1993. He is currently completing the M.S. degree in nuclear engineering at Illinois, studying fusion and plasma physics. He will continue research at Illinois for the Ph.D. degree in nuclear engineering.

Robert A. Stubbers received the B.S. degree in nuclear engineering from the University of Cincinnati, Cincinnati, OH, in 1994. He is currently completing the M.S. degree in nuclear engineering at the University of Illinois, Urbana-Champaign. His thesis research is concerned with pulsed operation of the cylindrical IEC.

Timothy A. Hochberg received the B.S. degree in applied physics from the California Institute of Technology, Pasadena, in 1989, and the M.S. degree in nuclear engineering from the University of Illinois, Urbana-Champaign, with a thesis on IEC plasma physics. Currently, he is nearing completion of the Ph.D. degree in electrical engineering at the University of Illinois, concerned with computational electromagnetics.

Jon H. Nadler received the Ph.D. degree from the University of Illinois, Urbana-Champaign, for work on early IEC experiments.

He was on the DOE Operations Staff, Idaho National Engineering and Environmental Laboratory, Idaho Falls, where he covered a range of projects involving both fission and fusion. He is currently a Professor of Physics at Richland Community College, Decatur, IL.

Robert A. Anderl received the Ph.D. degree in experimental nuclear physics from Iowa State University, Ames, in 1972. He is an Advisory Scientist with Lockheed Martin Idaho Technologies Company, Idaho National Engineering and Environmental Laboratory, Idaho Falls. His current research activities include experimental investigations of hydrogen/tritium interactions in plasma-facing component materials for the International Thermonuclear Experimental Reactor, and development of a sealed IEC neutron source for nondestructive materials evaluation applications.